Radio Astronomy at the Backyard: The Construction of a 11.7 GHz Radio Telescope and a 1420 MHz Phased Array Interferometer

Abstract

The essential goal of this project was that a typical – optically 'exclusive' – amateur astronomer could learn in practice the rudiments of radio astronomy, by means of constructing and using simple radio telescopes to be assembled with off-the-shelf materials within his reach. The idea was to capture some data from bright radio sources, and to assess the performance of the built instruments.

The total time lapse for this project spanned just three months (August- November, 2007). Two different operating frequencies were effectively tried: 11.7 and 1.42 GHz. For the former, one very simple radio telescope was constructed; for the latter, two much more sophisticated single units were built, with the final objective of attempting interferometry.

The construction and use of the simple 11.7 GHz radio telescope was a highly stimulating experience. It was easily assembled from totally common satellite TV components, and obtained outcomes largely overcame the more optimistic expectations. On the other hand, the building of the two 1420 MHz radio telescopes was hard, as it required the construction of very precise – and thus, highly time consuming – elements, while so far obtained results have been disappointing.

This report describes what has been done. It begins with a short presentation of the main equations of radio telescopes, followed by the description of the built instruments and their operation. Then, obtained radio data (basically, solar and lunar graphs) is shown, at the time that an interesting analysis of the lunar temperature variation with its phase cycle is presented. The report concludes with an appraisal of the main parameters of the constructed instruments, and a discussion evaluating the pros and cons achieved.

Introduction

A radio telescope measures the total radio power received from a source. If an astronomical source of radio waves falls within the 'beam' of a radio telescope, after proper processing, a dc voltage directly related to the strength of the incoming signal will appear at its output. "*It is rather like a one pixel eye looking at the heavens*" [1].

Likewise the main element in an optical telescope is the piece that collects the incoming optical photons – the *objective* or primary element – as it defines the potential performance of the whole instrument, the radio photons collecting dish – the *antenna* – of a single radio telescope represents its basic core.

The *acceptance* of the antenna is the angular region for which the antenna is sensitive. Quantitatively, it is defined as the solid angular area where the power received from a radio source is equal or greater than half the value obtained when the source is right on its central axis. For circular aperture antennas, the acceptance becomes a circle whose radius is called the solid angular *beamwidth* (q), and which is approximately given by [1] [2]

$$q = 1.019\frac{l}{D} \qquad (1)$$

where l is the *wavelength* of the incoming radiation and D is the *diameter* of the aperture. The larger the diameter, the narrower the beamwidth and the smaller the acceptance.

The *spectral power density* (P) collected by a radio telescope from a given radio source to whom it is pointed to becomes [2]

$$P = \frac{1}{2}hAF \qquad (2)$$

where h represents the *efficiency* of the dish, A is the *geometrical area* of the dish, and F is the *flux density* of the considered radio source.

The factor 1/2 arises because the antenna can receive electromagnetic radiation of just one polarization at the time of the usually two (*circular polarization*) that the flux density of astronomical sources actually carries.

Using the analogy that a resistor at *absolute temperature* T produces a spectral power density given by

$$P = k\,T \qquad (3)$$

[1] Small corrections are required to the 1.22 factor of the original Rayleigh criterion formula, as this applies to a slit rather than a circular aperture.
[2] All formulas presented in this section have been extracted from the following references: [3, 4, 5].

where *k* is the *Boltzmann's constant*, by equating (2) and (3) it is possible to express the flux density of a given radio source collected by the dish of the radio telescope into units of a fictitious temperature, so that

$$T_A = \frac{hAF}{2k} \tag{4}$$

where the temperature T_A, *the brightness temperature of the source detected by the antenna* (or simply *antenna temperature*), represents a quantitative equivalent magnitude of the effect of the considered radio source on the dish of the radio telescope in question.

In case that the considered astronomical source radiates just thermal radiation, that is, it behaves like a perfect blackbody of absolute temperature *T*, its total *brightness* (*B*) becomes given by the *Planck's radiation law*

$$B = \frac{2h\nu^3}{c^2}\frac{1}{e^{h\nu/kT} - 1} \tag{5}$$

where *h* is the *Planck's constant*, ν is the *frequency* of the radiation, and *c* is the *velocity of light in vacuum*.

Whereas $h\nu << kT$, which particularly applies for the case of radio frequencies, the general case of (5) can be simplified (*Rayleigh-Jeans law*) as

$$B = \frac{2h\nu^3}{c^2}\frac{kT}{h\nu} = \frac{2\nu^2 kT}{c^2} = \frac{2kT}{\lambda^2} \tag{6}$$

Considering that the flux density equals the brightness times the solid angle subtended by the source (Ω), that is $F = B\Omega$, then by replacing it in (4) and (6) it becomes

$$F = \frac{2kT_B\Omega}{\lambda^2} \Rightarrow T_B = \frac{\lambda^2 T_A}{hA\Omega} \tag{7}$$

where T_B represents the *real brightness temperature* of the considered blackbody radiator. In such context, the radio telescope is called a *radio thermometer* or *radiometer*.

In practice, the process of measuring T_A necessarily includes contributions (distortions) from some other agents, as in addition to the excitation from the source, others non zero temperatures must be taken into account. Thus, what in practice could be measured is not T_A alone but the whole *system temperature*:

$$T_{sys} = T_A + T_R + T_{sky} + T_{gnd} \tag{8}$$

where T_R represents the contribution due to the *receiver noise temperature*, T_{sky} is the contribution due to the *sky temperature* (the temperature corresponding to sky adjoining the considered target, as radio sources are typically much more smaller than the telescope

beamwidth), and T_{gnd} is the contribution from the ground (*spillover temperature*). Regarding that T_{sky} can be properly estimated, having $T_R + T_{gnd}$ as low as possible translates as lesser errors in finding T_A. It is usually convenient to work with the *equivalent noise temperature* of the overall radio telescope (T_N), defined as

$$T_N = T_R + T_{sky} + T_{gnd} \quad = T_{sys} - T_A \tag{9}$$

The *energy source per second* (p_S) passing from the dipole through the system exclusively due to the radio source is given by

$$p_S = k\, T_A\, \Delta u \tag{10}$$

where Δu is the receiver frequency bandwidth [3]. Thus, the *signal power* (P_S) arriving at the diode detector after amplification by the radio receivers exclusively due to the radio source is given by

$$P_S = G\, k\, T_A\, \Delta u \tag{11}$$

where G is the total gain of all receivers.

As already seen, in practice there is always an unwanted *noise power* (P_N) associated with noise generated from within the receivers. This adds in an unwanted power given by

$$P_N = G\, k\, T_N\, \Delta u \tag{12}$$

and hence, the real *total power* (P_T) arriving at the input of the detector diode is

$$P_T = G\, k\, T_{sys}\, \Delta u \tag{13}$$

where T_{sys} has been introduced applying (9).

The real total power arriving at the input of the diode detector can also be expressed as

$$P_T = V_i^2 / R \tag{14}$$

where V_i is the input voltage to the diode, and R is the system resistance (nominally the same value as the impedance of the connected elements). Combining this two last equations,

$$V_i = \sqrt{G.k.T_{sys}.\Delta u.R} \tag{15}$$

The effective noise temperature of the receivers fluctuates due to the random nature of the movement of the electrons in them. As it is a randomly generated variation, the effect of the variation in the radiometer's final temperature measurement can be reduced by averaging the noise signal over a greater bandwidth and by integrating the final dc voltage over many

[3] The frequency bandwidth is usually measured between the output frequencies whose signal strength is half the maximum when the in put signal power is constant with frequency [6].

readings. Thus, the random fluctuation in the noise temperature can be reduced to its minimum possible value given by the expression

$$\Delta T = \frac{T_N}{h\sqrt{t\Delta u}} \tag{16}$$

where t is the *time constant* of the integrator smoothing the detected dc voltage. This sets the minimum temperature change that the radio telescope system will respond to, so that ΔT essentially defines the *temperature resolution* of the radiometer. Logically, it depends on the quality of the instrument (the lower the noise temperature, and the greater the efficiency, the time constant, and the frequency bandwidth, the better the temperature resolution).

The *minimum detectable source flux density* (S_{min}) for a full power radio telescope has to deal with its temperature resolution and antenna dimensions, thus resulting

$$S_{\min} = \frac{2k\Delta T}{A} = \frac{2kT_N}{Ah\sqrt{t\Delta u}} \tag{17}$$

Summarizing, in order to maximize the detected signal and the overall performance of any considered radio telescope, it is required that:

- it maximizes the bandwidth
- it has long integration time constants to smooth the signal output
- it has a large dish and efficient a well matched feed dipole
- it minimizes the noise temperature of the system

Considering that square-law diode detectors are frequently used in radio telescopes to recover signals immersed in the system noise (although "*their use is commonly restricted to narrow dynamic ranges of very low signal levels where the square law is valid*" [7]), this fact makes that the dc output voltage (V_o) results proportional to the input power, so that

$$V_O \propto P$$

This important "empirical" relation now leads to the conclusion that V_o (the actual outcome from the radio telescope) results proportional to $T_{sys,}$ *all other factors being constant*. V_o can be measured with a voltmeter, chart recorder or an ADC connected to a computer. Then, it becomes

$$V_O = K_{sys} T_{sys} \tag{18}$$

Therefore, by using two measurements from different sources (source #1 and source #2), the unknown coefficient K_{sys} can be eliminated as

$$\frac{V_{O1}}{V_{O2}} = \frac{K_{sys} T_{sys1}}{K_{sys} T_{sys2}} = \frac{T_{A1} + T_{N1}}{T_{A2} + T_{N2}} \tag{19}$$

The built radio telescopes

Two different operating frequencies were selected for this project: 11.7 GHz and 1420 MHz. The first one because of the readiness of required materials, the second one because it is a fundamental frequency in astronomy – it is the frequency of the line emission of the most abundant element in the whole Universe: neutral hydrogen. Even at the amateur level, serious studies could be promisingly undertaken for the 1420 MHz system.

Therefore, the 11.7 GHz radio telescope was conceived to be merely used for this project as an educational tool for learning the rudiments of practical radio astronomy. Conversely, the 1420 MHz system was much more ambitiously devised, regarding it as a valuable long term instrument for serious research at the amateur level.

Figure 1
A general view of the northern facade of the observatory after embracing the radio experience.

The 11.7 GHz radio telescope

As Figure 2 shows, the 11.7 GHz radio telescope is a very simple instrument. Outdoors there are just the antenna and the *low noise block* converter (LNB), while indoors there are the line amplifier, the receiver, the analogue to digital converter (ADC), and the PC [8, 9, 10, 11].

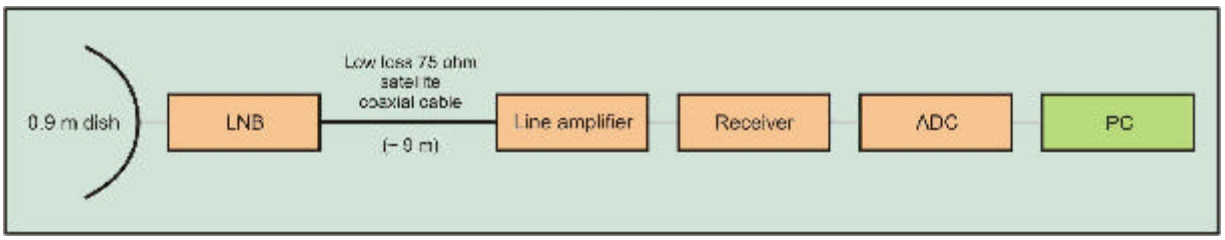

Figure 2
The block diagram of the simple 11.7 GHz radio telescope.

The antenna is an almost circular (91-99 cm) second-hand standard offset dish for satellite TV *Ku band* (Figure 1, near the centre between the large dishes). Although it has no motor, it is fully steerable in the vertical and horizontal planes by hand. For reading the altitude angle (elevation) it already had a graded scale (Figure 3), while a simple one was incorporated just for reading the azimuth angle (Figure 4).

Figure 3
The original elevation scale.

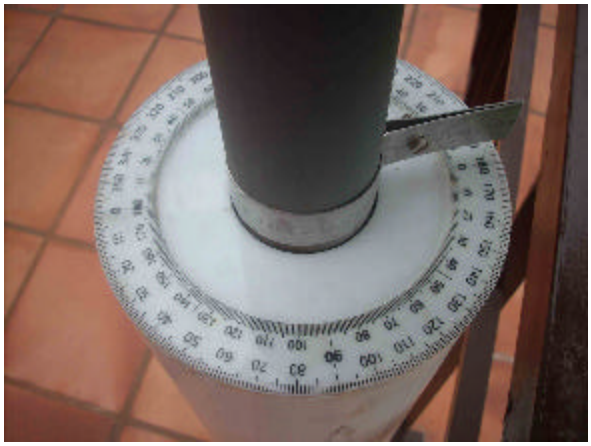

Figure 4
The adopted azimuth scale.

The LNB is also a standard satellite TV component (it came with the dish). It has an operating range from 10.7 to 12.75 GHz, a 65 dB gain, a noise figure of 0.7 dB, and its down converted output is from 950 to 1,950 MHz, at 75 ohm. It is fed through the output coaxial cable at 15 V.

The outdoors-indoors connection is made via 9 m of a 75-ohm RG06/U coaxial cable. Its attenuation at 1,000 MHz is 21.46 dB per 100 m [12]. All connectors are F type.

The line amplifier is a standard satellite TV wide line amplifier, 950 – 2250 MHz, 20 dB, 75 ohm, 15 Vdc (fed through the coaxial lead from the receiver).

The receiver was originally a standard *Satellite Finder* (Figure 5), a simple instrument used by TV technicians to facilitate the correct alignment of TV dishes at field[4]. It has to be modified (Figure 6) due to two reasons: (a) to obtain a fine variable gain, and (b) to feed the line amplifier and the LNB through the coaxial cable itself.

The modifications performed on the satellite finder are presented in Appendix I. Its original potentiometer – identified by the label "dB" at its front – actually works adjusting the threshold of the rectified signal to be amplified by the operational circuits – sort of *noise squelch function* – and the variable gain is properly adjusted by an especially new added potentiometer [13]. The satellite finder requires 15 Vdc from a regulated power supply.

[4] The Satellite Finder takes the signal that comes from the output of the LNB, and after proper amplification and rectification, it presents the corresponding signal strength on an analogue meter at its front. This allows that after a rough initial orientation of the dish towards the satellite in question, the precise alignment is rapidly achieved just by moving the dish until obtaining maximum needle displacement.

Figure 5
The original satellite finder device.

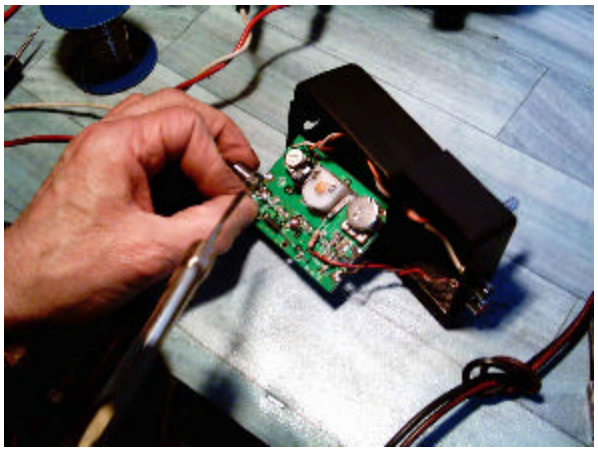

Figure 6
Modifying the satellite finder.

The electrical parameters of the modified satellite finder are: operating band 950 to 1450 MHz, 17 dB of RF gain, diode detector, an integration time constant about 0.1 sec, 40 dB of variable DC gain, 0 -7 Vdc output, 75 ohm input.

The backend is completed with the ADC and the PC (Figure 7). The ADC is based on the MAX186ADC integrated circuit. It is a 12 bit device, has 8 channels, a full input range from 0 to 4.095 V at a sample rate of 133 kHz, and RS232 output to enter into the PC [14]. The software is *SkyPipe Pro* version [15], working under *Windows Xp*. This software is a typical recording chart program but especially designed for working with the MAX186ADC integrated circuit. It expresses the input voltage at the ADC directly in millivolts.

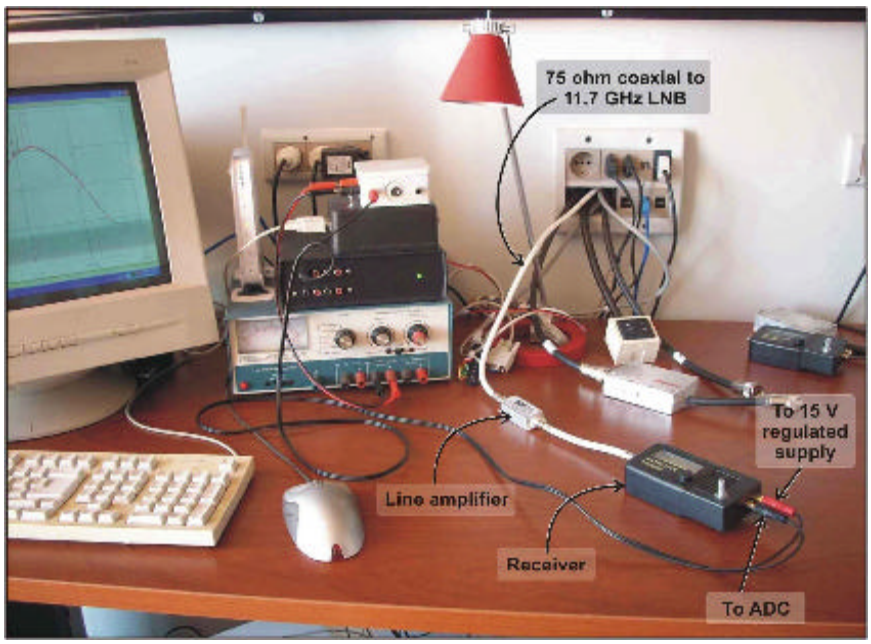

Figure 7
The complete backend of the 11.7 GHz radio telescope, actually collecting the graph shown in the PC.

The 1420 MHz radio telescopes

The block diagram of both 1420 MHz radio telescopes, connected together in order to perform as a drift *phased array* interferometer, is shown in Figure 8. Each frontend comprises the dish, the half wave dipole, the low noise amplifier (LNA), and the filter; both frontends are identical. The backend includes the adder/impedance matcher, the line amplifier, the receiver, the ADC, and the PC [16, 17, 18].

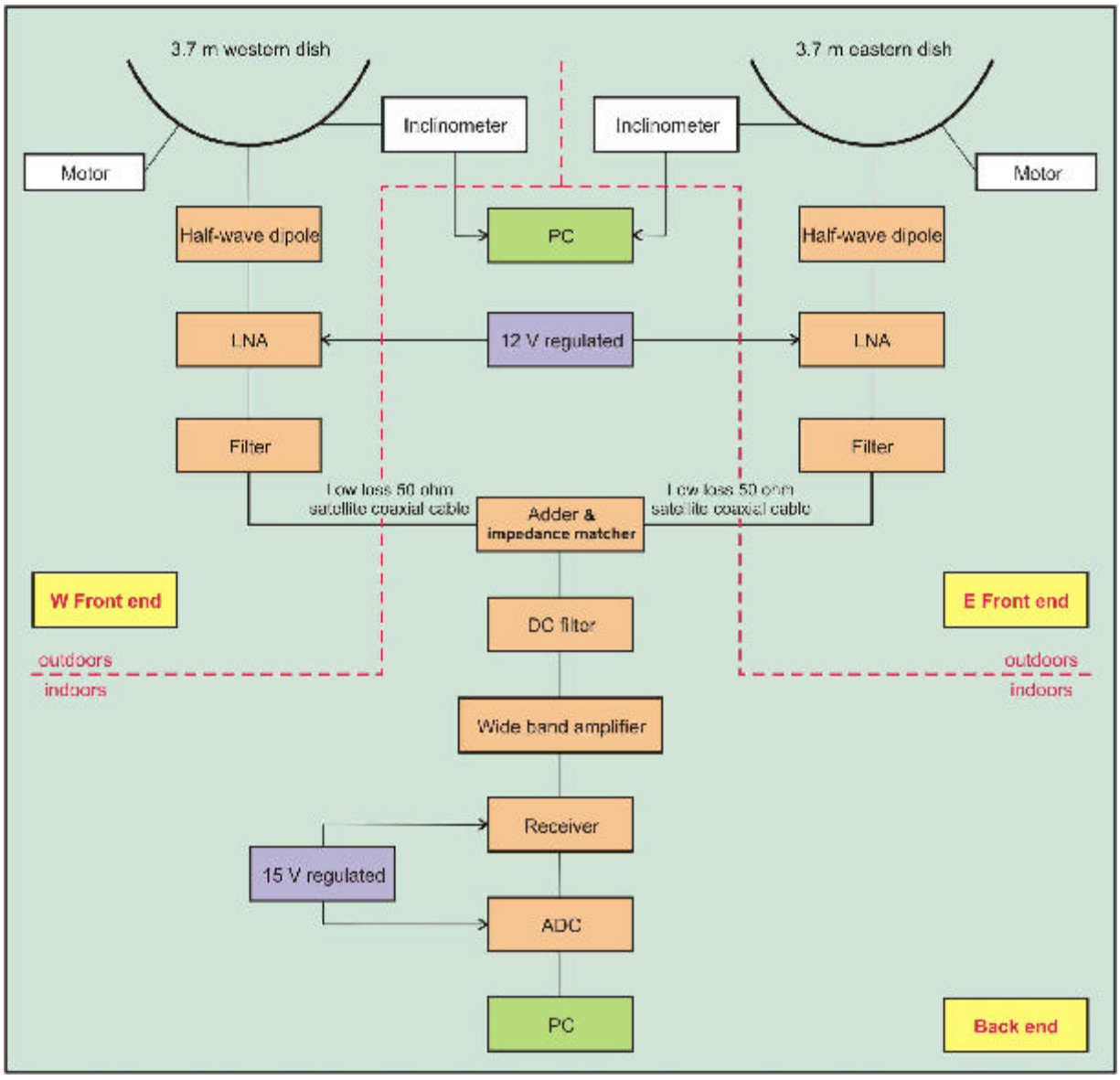

Figure 8
The complete block diagram of the constructed 1420 MHz phased array interferometer. Except for the adder & impedance matcher, and the DC filter, the backend is exactly the same as for the previously discussed 11.7 GHz radio telescope.

Figure 9
The identical 3.7 m antennas for the phased array: the W at left, the E at right.

The dishes (both second-hand *Paraclipse*, model 12, shown in Figure 9) have a diameter of 3.7 m of diameter, a focal length of 2.6 m (thus f/D = 0.7), and have been placed 19 m apart along the east-west direction. Both antennas can only be moved on the meridian, by means of slow 12 V motors that are commanded from indoors. Electronic inclinometers (*Smart Tool Technologies*, model ISU-S) with an accuracy of $\pm$ 0.1 degree, connected via RS232 to an indoor PC, permits to know the precise elevation angle of each antenna.

The two required 1420 MHz half wave dipoles (Figure 10) have been especially constructed for this project, according to exact dimensions included at Appendix II. Each device has to be placed in order that the focus of the dish precisely lays on-axis, half way between the dipole and the backing disc. The expected bandwidth is about 75 MHz (it was not measured yet).

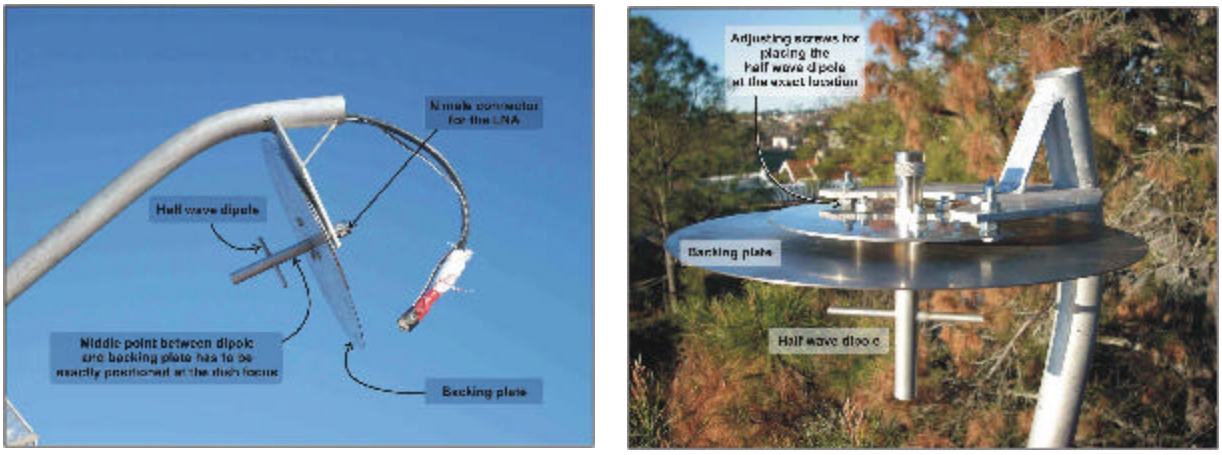

Figure 10
The 1420 MHz half wave dipoles have been constructed according very precise dimensions.

The 1420 MHz LNAs (*Radio Astronomy Supplies*) are the only elements used along this project that neither were standard satellite TV surplus components, nor were made by the author. These LNAs, particularly designed and constructed to work for radio telescopes, have a gain of 28 dB at noise figure of 0.34 dB, 50 ohm, N connectors, and require 100 mA from an external 12 Vdc regulated power.

The 1420 MHz resonant mechanical filters (Figure 11) have also been made for the case, according to exact dimensions included at Appendix III. Both filters were adjusted for minimal attenuation at 1420.0 MHz. One presents an attenuation of 4.2 dB and a 26 MHz passband (from 1408 to 1434 MHz), while the other has 3.8 dB and a 78 MHz passband (from 1364 to 1442 MHz).

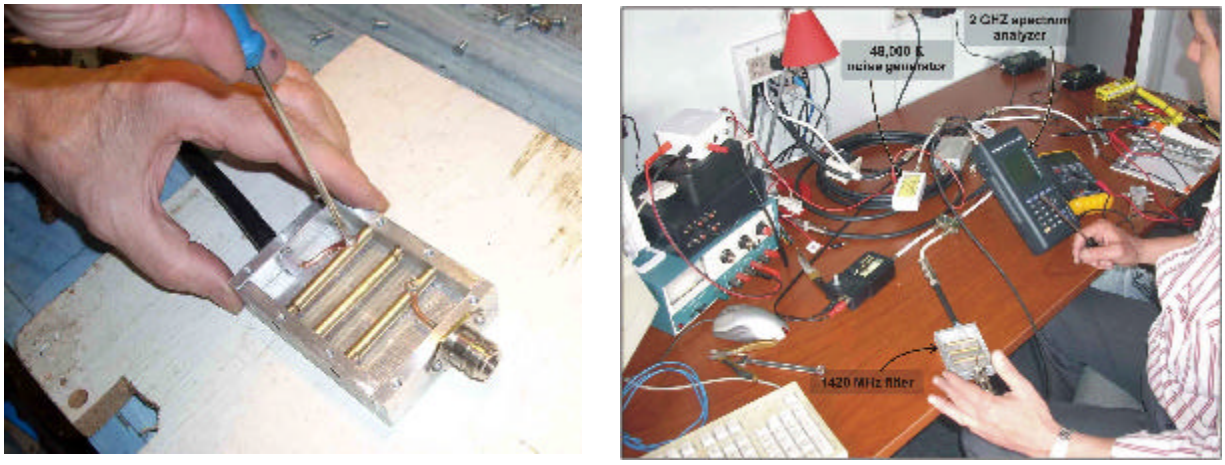

Figure 11
At left, finishing the assembling, at the exact required dimensions (the copper rods and air gaps act like inductances and capacitors). At right, adjusting the filter at bench, with a noise generator and a 2GHz spectrum analyzer, in order to center the passband at exactly 1420 MHz by tweaking the gaps.

The used coaxial cable is a low loss 50 ohm 8D-FB type. Its rated loss at 1,000 MHz is 4.50 dB per 30 m [19]. All connectors used are N type. The length of the coaxial cable to the eastern antenna is 16.20 m, while for the western one is 21.17 m. For the correct phased array operation, a coaxial cable supplement of 4.97 m is added at indoors to the former in order to obtain perfect phase matching [5]. For just single operation, the shorter length of the eastern antenna can be conveniently use.

As its name implies, the adder/impedance matcher has two purposes to fulfill at the same time: (a) to join together the signals from both antennas at 50 ohm, and (b) to match the output to 75 ohm. The practical solution to this problem is shown in Figure 12. After the

[5] The length of the cables has to be normally cut to better than 10% accuracy (ie 2cm for 20cm wavelength) if the fringes are required to not be phase shifted with respect to time. That is, if the lengths differ, all that will happen is that the maximum will occur at a displaced time (say at 11:50 am or 12:10 pm instead of exact 12:00 eg for a proper observation of the sun at midday). Inaccuracies do become important for a variable base line interferometer (producing different sets of fringes) when it is required to add all the fringe patterns from the different base line separations together. Correct phasing for *aperture synthesis* is absolutely essential [20].

soldered joint of the two 50 ohm coaxial cables, there is still a 50 ohm short run (actually 3.5 cm) before meeting the 75 ohm cable (diagram and computations at Appendix 5).

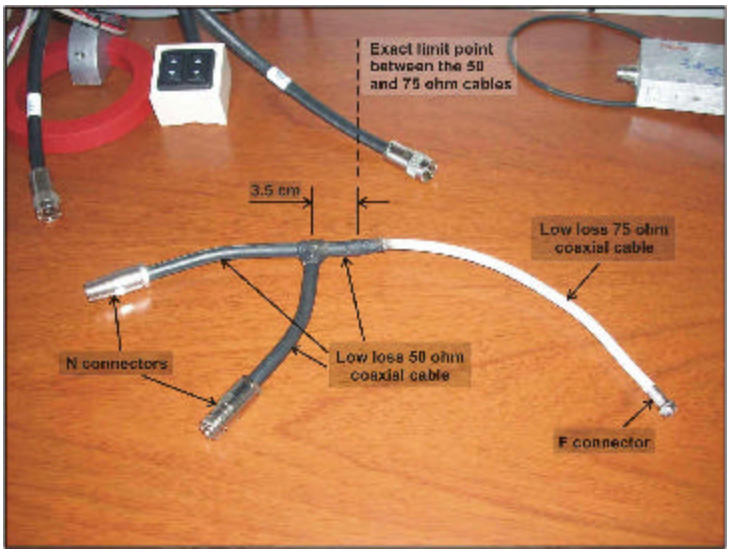

Figure 12
Signals from each antenna are directly added, and impedance then changes from 50 to 75 ohm.

The line amplifier, the receiver (modified satellite finder), the ADC, the software and PC are exactly the same as for the previously described 11.7 GHz radio telescope. Figure 13 shows the actual connections for the 1420 MHz operating as a single radio telescope (at left), or as a phased array interferometer (at right).

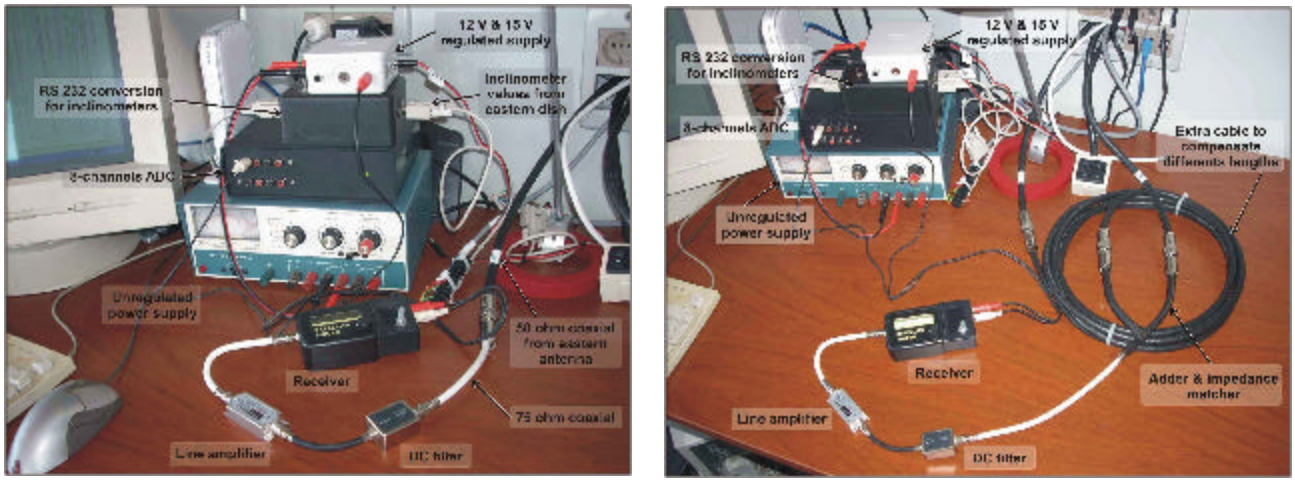

Figure 13
At left, the configuration required for performing as a single dish 1420 MHz radio telescope, using the more convenient (nearer) eastern antenna. At right, the configuration required for performing as a phased array interferometer (besides the adder, extra cable is needed for compensate different coaxial lengths).

Operating the radio telescopes

The first task performed with the 11.7 GHz radio telescope was to learn how to properly point it to the desired radio target. As the LNB is placed off axis, the usual straightforward method of making its shadow to appear right at the dish's centre was obviously useless.

Working with the Sun's signal (the strongest and easiest one), by trial and error it was found out that the maximum output signal corresponds when the dish is positioned at exactly 8.5 degrees above the altitude angle of the celestial radio source – readily obtained from a planetarium software – measured on its vertical scale (Figure 3). Such angular displacement was verified to be the same for all possible elevations.

The next step was to learn how to set the potentiometers of the modified satellite finder for obtaining a proper output. On the one hand, this means that the dc output should stay at its lowest value when there is no radio source within the radio telescope beamwidth; on the other hand, when a radio source is actually present, the dc output should not overflow the following ADC unit. This setting depends on both the particular selected target and reigning conditions at that moment. The right proceeding was found to be the following two steps method:

- Firstly, the dish has to be pointing to open sky, and the 'gain' potentiometer positioned just at middle way. Next, the 'squelch' potentiometer has to be slowly turned clockwise until the needle barely deflected, and then, turning it backwards as minimum as required for leaving the needle again in repose.

- Secondly, the dish has to be pointing directly to the radio source in question. Without touching the squelch pot, the idea is to adjust the gain pot in order to obtain the largest possible dc output that still does not saturate the ADC unit – that is, it should remain always under 4.095 V, which can be easily checked in the corresponding graph.

One thing worth mentioning is that every time the 11.7 GHz system was turn on (that is, after the LNB became fed) the dc output of the satellite finder immediately went to its maximum, and then began to decrease very slowly – not matter where the dish was pointing to, or whether the LNB had been working very recently. The complete stabilization normally took about 45 minutes. The justification for this behaviour is yet not understood.

In the case of the 1420 MHz system, there was an important task to be performed before the described proceeding could be applied. Unlike the former case, where the LNB had already been placed at its right location – such dish and LNB had been normally operating and never became disassembled – the half wave dipoles had to be precisely positioned at the right focus of the large dishes.

This implied to axially move the central tube which supports the half wave dipole so that it becomes closer or farther apart the dish, until the focus precisely laid on-axis, half way between the dipole and the backing disc. In practice, this was performed by exactly pointing to the Sun when three little mirrors had been strategically placed on the mesh, without distorting its shape. Incidentally, by changing the position of the mirrors it was also possible to corroborate the correctness of the parabolic shape. Considering that deviations up to ~ 2 cm (l /10) are totally acceptable [21], both dishes are in 'very good shape'.

First radio graphs

On October 20, 2007, after proper installation, alignment, and adjustments, and despite it was (lightly) raining all day long, the very first radio graphs were finally obtained from this amateur facility [6]. Figure 14 shows the solar transit captured by the 11.7 GHz radio telescope.

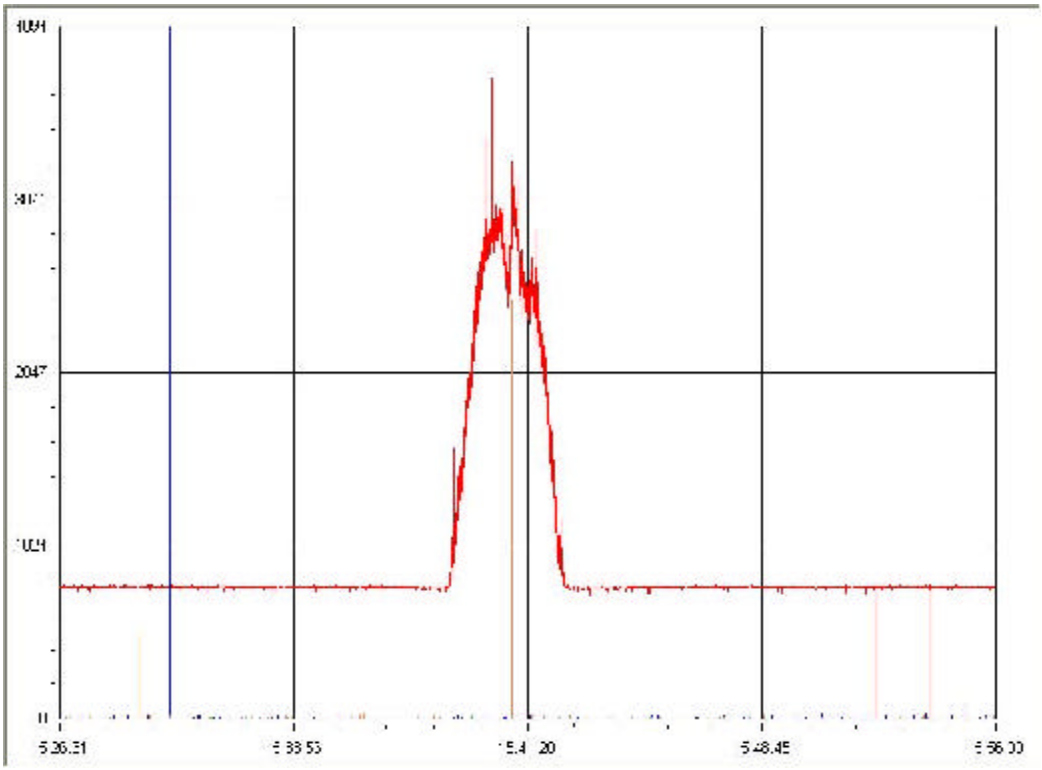

Figure 14
The 11.7 GHz radio signal from the Sun while it was (almost) transiting by the observation facility on Oct 20, 2007, at 15:40 UT.

As the signal from the Sun is so strong, it was necessary to work without the line amplifier (just the LNB directly connected to the modified satellite finder). Even in this configuration, the 'squelch' pot had to be placed not right at the threshold value but well below it, as otherwise there was no remedy for saturation at the maximum signal. The consequence is clearly visible in the abrupt raising and declining of the curve. The total curve elapsing time is 226 seconds.

Some few hours later, with the Moon favourably located at the sky, it was also possible to obtain valid lunar graphs after proper adjustments. Considering that the 11.7 GHz radiation from the Sun is about 100 times larger to that from the Moon (the corresponding graph is

[6] The excitement provoked on the author by these real first-captured radio graphs was only comparable to the satisfaction achieved on occasion when the anxiously observed dc voltage output of the radio telescope clumsy began to react for the first time, whenever the dish was pointing to anything but the open sky.

included in Appendix IV), those required 20 dB of extra gain were supplied by means of adding a line amplifier.

Figure 15 shows the first lunar graph obtained. Compared to the solar curve, it is readily noticed that the lunar graph appears very different, as (a) it gradually raises and sets from the rest level, and (b) it shows a much lesser level of variability. In this case, the total curve period is 683 seconds. Given the gentle rise and decline, such high quality response intimately corresponds to the dish beamwidth (the computation is in the following section).

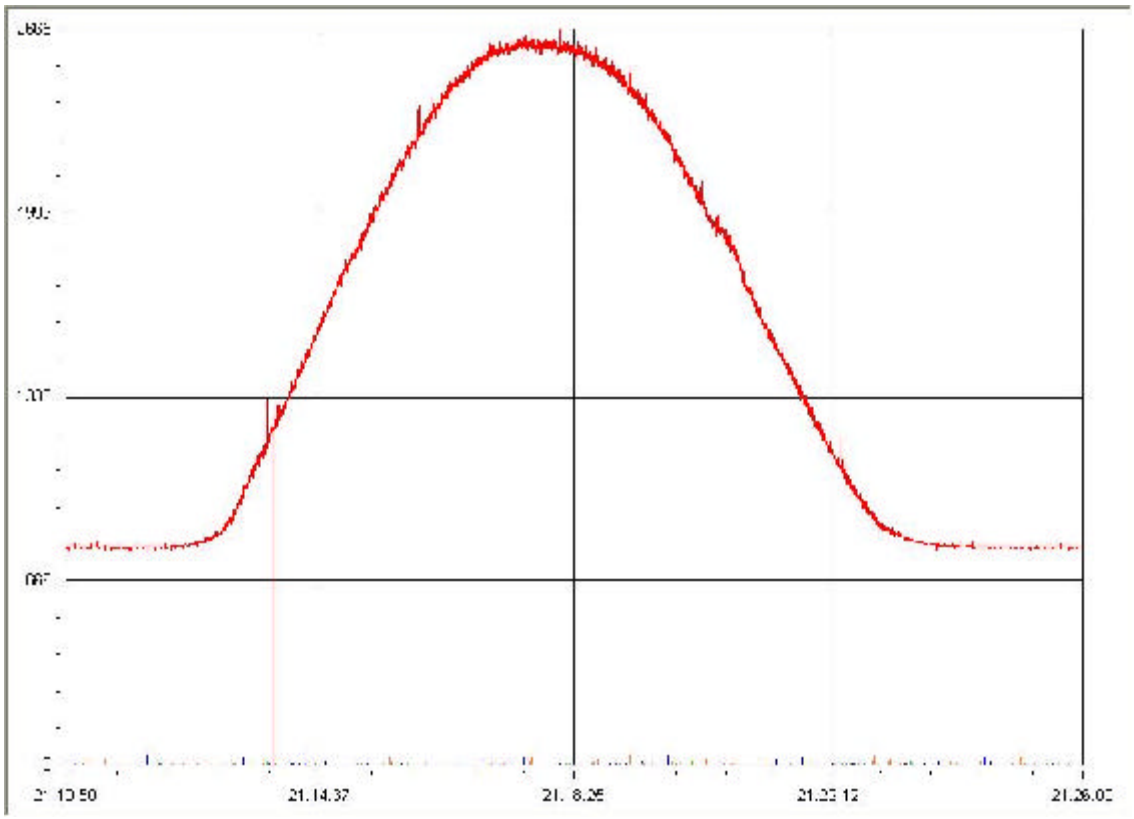

Figure 15
The 11.7 GHz radio signal from the Moon on Oct 20, 2007, at 21:18 UT.

The first radio graphs from the 1420 MHz radio telescope (actually from the eastern single antenna) were obtained on October 28, 2007. Figure 16 presents the document of the solar transit of that day (in reality, it occurred 15:35 UT), captured simultaneously by the 1420 MHz (in red) and the 11.7 GHz (in blue) radio telescopes.

The solar radio graph at 1420 MHz appears much more noisy that at 11.7 GHz, denoting that there is much more local interference at the former frequency. Regarding that the noise squelch adjustment for each receiver was arbitrarily set, nothing can be said about the

relative signal strength at each frequency [7]. On the other hand, the notoriously different elapsing times (about 878 and 314 seconds, respectively for the 1420 MHz and 11.7 GHz cases), denotes that the beamwidth of the 1420 MHz radio telescope would be considerable wider than the beamwidth of the 11.7 GHz.

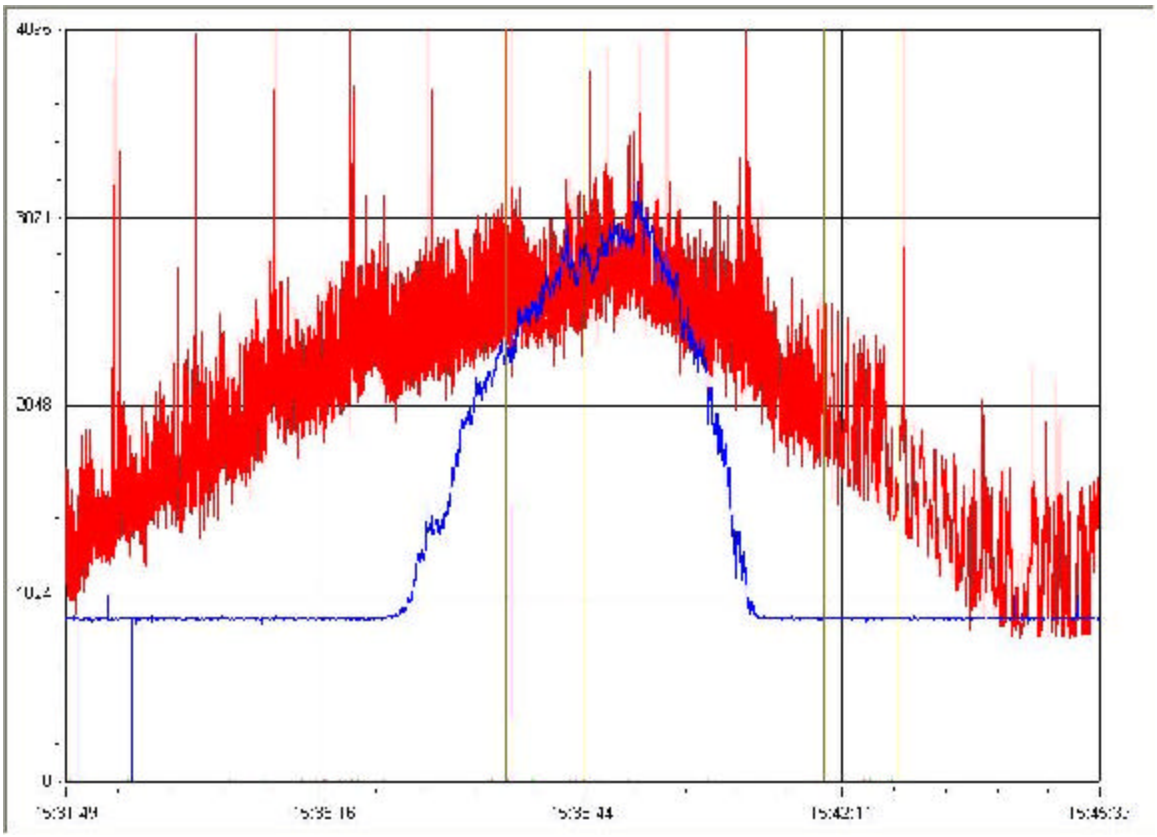

Figure 16
The solar radio graphs at 1420 MHz (red) and 11.7 GHz (blue) collected simultaneously while (almost) transiting on October 28, 2007, at 15:39 UT.

Considering that there was not much activity on the solar surface at the time of the observations (the solar cycle is presently going about its minimum), it would be interesting to investigate what was actually causing the variations detected while the Sun was being mapped. At the time of this writing, this is still an open matter.

Finally, despite all the attempts performed to obtain any observable interfereometric outcome from the phased array pointing to the Sun (the greatest astronomical source at 1420 MHz), no one single fringe ever appeared. It was tried filtering either at each frontend (as described) or at indoors, without any filtering, adding another line amplifier (and even a third one, which resulted completely useless as there was no way to stop oscillation), eliminating the line amplifier, and all possible combinations among them. The invariable outcome was always noise, just noise, and nothing more but noise.

[7] As the graph of *"The Strongest Radio Sources"* on Appendix IV presents, the flux density for the quiet Sun at 1420 MHz is about as half as for 11.7 GHz.

Lunar radio graphs

Lunar 11.7 GHz radio graphs were obtained from the *Observatorio Los Algarrobos, Salto, Uruguay* (31º 23' 31.5" S, 57º 58' 41.5" W) during nine observing sessions, covering a total period of 15 days (from October 20th to November 4th, 2007). Missing days were due to electrical storms. A minimum of five graphs were attempted at each observation session, although several graphs had to be rejected due to interference. Incidentally, a few points at the sky where the strength of the 11.7 GHz signal was moderate to high appeared unexpectedly (most likely, due to satellites emitting TV signals).

Figure 18 shows several of the collected lunar graphs. The totality of obtained data is contained in the table presented in Appendix V.

All data was collected by using the same equipment. In particular, the indoors devices also operated basically under the same environmental conditions (permanent air conditioning). The used modified satellite finder was always the same; its gain setting was never modified, while the noise squelch potentiometer was barely readjusted only twice or thrice.

For each graph it was measured the maximum dc voltage obtained, the voltage base level, the total time from the initial detection of the raising edge to the last moment of the trailing merge, and the time lapse of the curve full width corresponding to the value equal to half its maximum (FWHM). The use of the FWHM was preferred to the total curve time due to representing the actual drifting time much more accurately, especially considering that some graphs were moderatlely asymmetric.

Different total drifting times (or different FWHMs, as they are intimately related), denote that lunar drift paths in front of the beamwidth of the 11.7 GHz radio telescope were also different – something most likely to expect, considering the broad $\pm$ 1º pointing accuracy.

Figure 17 examples such situation. In case the Moon drifted by the AB path, its drifting time is clearly different compared to, for instance, the CD path. In practice, things are more complicated, as the beam of the dish is two dimensional but not necessarily symmetric, so the actual shape of the acceptance instead of a neat circle could perfectly be an ellipse.

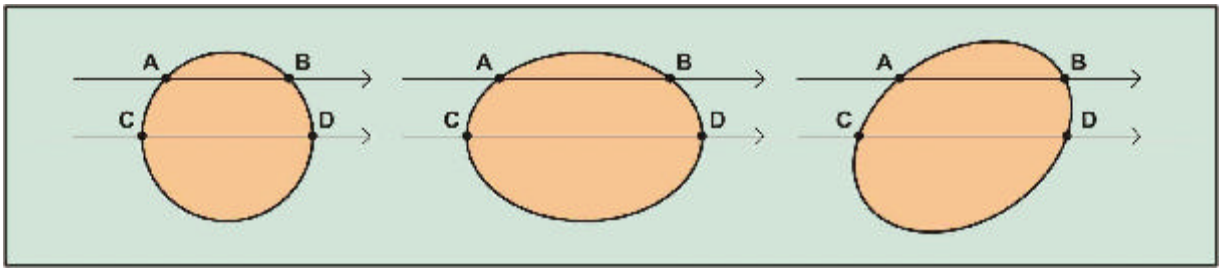

Fig 17
The drifting of the radio source in front of the beamwidth of the radio telescope. Drifting times depend on the real traveled path, and also on the actual shape of the beamwidth. Even worst, real drifting paths are not straight lines (as shown), but arcs.

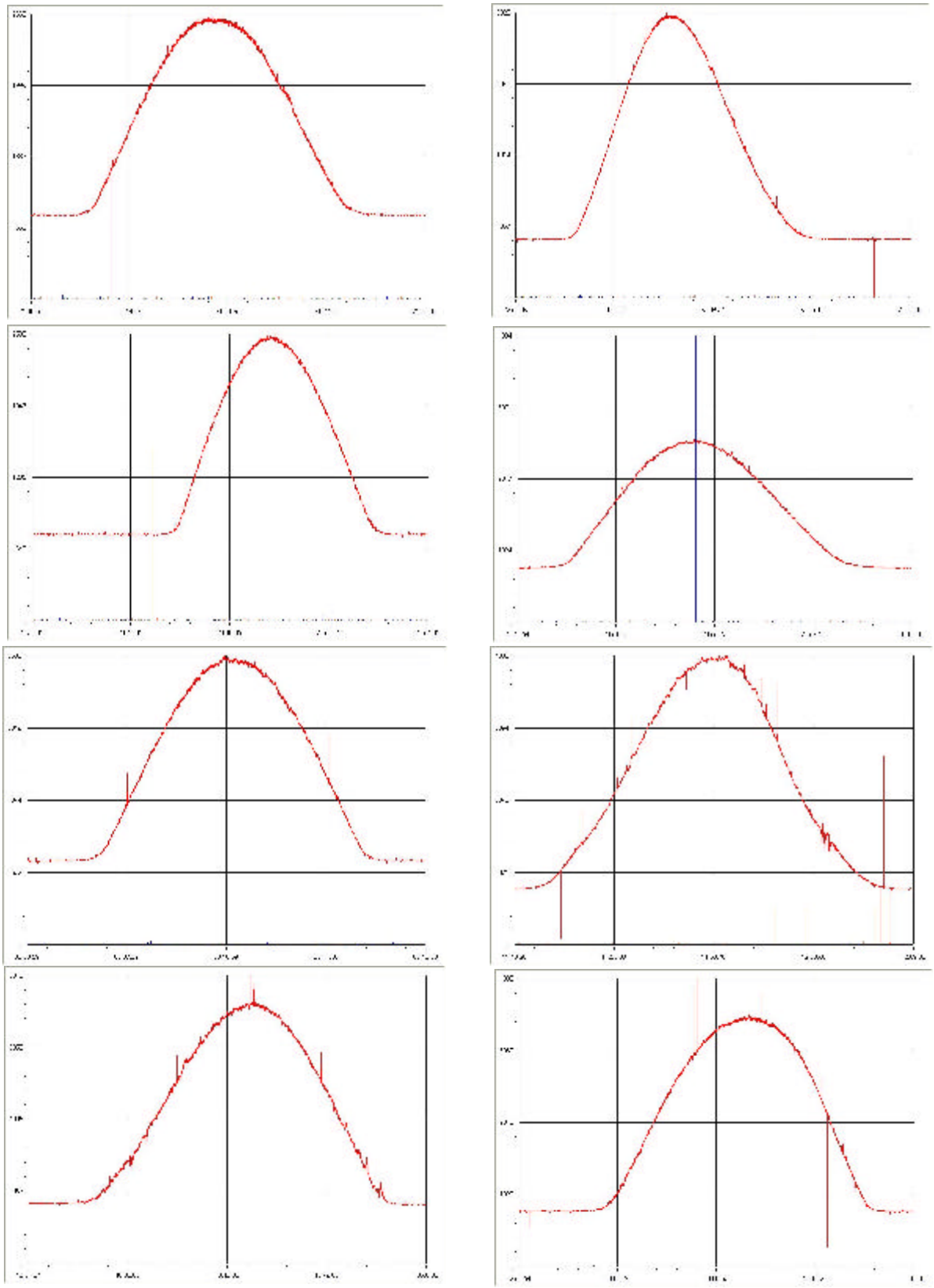

Fig 18
Lunar graphs at 11.7 GHz obtained on the following days (from upper left to bottom right): (1) Oct 20, (2) Oct 21, (3) Oct 23, (4) Oct 24, (5) Oct 28, (6) Nov 2, (7) Nov 3, and (8) Nov 4.

The different FWHMs *"are due to the fact that the moon is not moving through an identical part of the beam everytime. The beam of the dish is not itself perfectly symmetrical (even if the dish is) due to the way that the feed dipole in the LNB matches to the dish"* [22].

As the maximum dc voltage output (V_{max}) depends on for how long the Moon actually drifted in front of the beamwidth, maximum dc voltages per se do not represent the real strength of the considered radio signal. However, in case the FWHM – V_{max} relation were known for a given signal strength, from measured (FWHM, V_{max}) pairs it could be found out if the radio source at that time was either higher, equal, or lower, than the reference one.

Plotting observed FWHM drifting times against measured V_{max} for all accepted graphs it is readily noticeable a strong correlation, as seen in Figure 19, which can be properly represented by the equation

$$V_{max} = 7.019\ x\ (\text{FWHM}) + 268.01 \qquad (20)$$

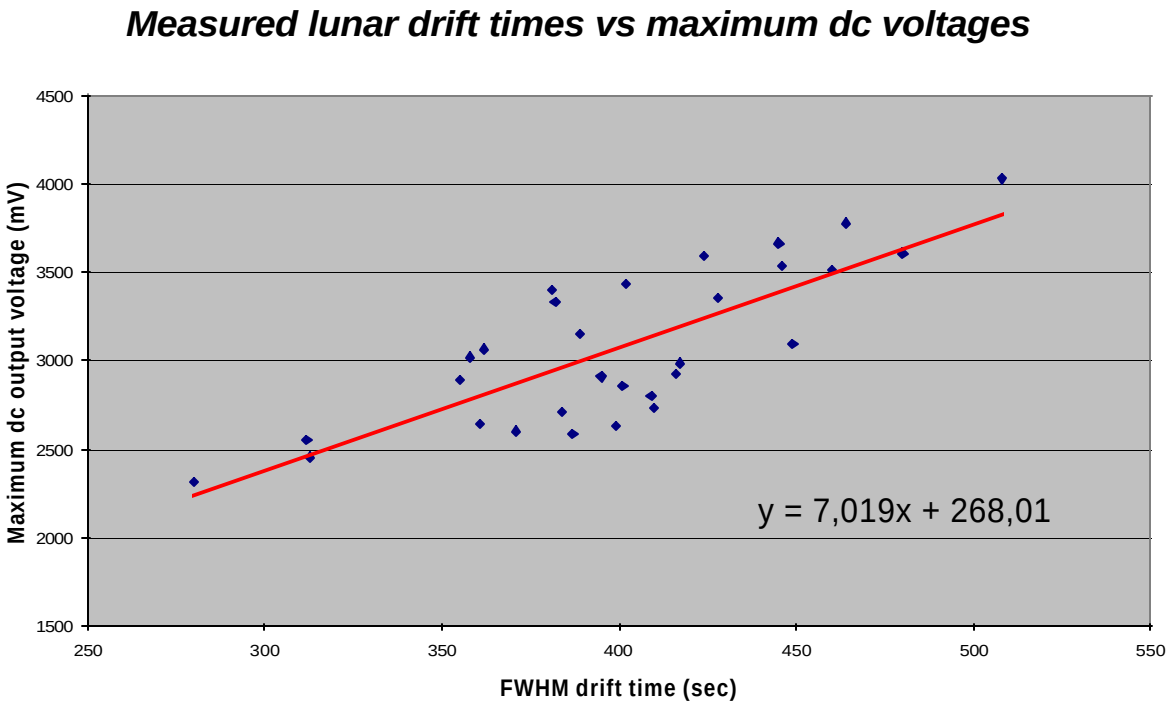

Fig 19
The plotting of all accepted data from the nine observing sessions, showing a strong correlation, whose analytical expression appears at the bottom right of the graph.

Then, for each observing session it was calculated the *average* V_{max} and the *average* FWHM. By applying equation (20) to this latter value, it was possible to obtain the dc voltage output that would have corresponded in case the lunar 11.7 GHz radio emission were always of the same strength ($V_{formula}$). Finally, by subtracting those values (the average V_{max} minus $V_{formula}$) a quantitative indicator of the relative strength variation of the lunar radiation at the observed frequency, for the considered period, was able to be found.

The following table summarizes the data in question:

Date of observation	***Moon age (days)***	***V_{max} (av) (mV)***	***FWHM (av) (sec)***	***$V_{formula}$ (mV)***	***$V_{max} - V_{formula}$ (mV)***	***Error $V_{formula}$ (mV)***
2007-10-20	8,9	2617	385	2970	-354	139
2007-10-21	10,0	3320	433	3304	16	313
2007-10-23	12,2	2596	317	2491	104	237
2007-10-24	13,4	3304	435	3321	-18	271
2007-10-28	17,0	3213	389	2996	217	226
2007-11-01	21,7	2968	386	2975	-7	184
2007-11-02	22,7	3396	455	3460	-64	270
2007-11-03	23,7	2983	398	3064	-81	91
2007-11-04	24,7	3128	402	3088	40	277

The last column at right represents the error of the corresponding dc output voltage obtained by applying (20), given the dispersion of the different FWHMs supporting the corresponding average FWHM. The actual computation for each value was

Error = 7.019 *x (standard deviation of considered* FWHMs)

where the factor 7.019 is the angular coefficient of (20).

According to (17), the measured dc output directly relates to the power of the radio signal input and consequently to the temperature of the blackbody radiator. Therefore, the detected variation of the $V_{max} - V_{formula}$ values as the Moon's cycle aged also represents the way the lunar radiation at 11.7 GHz varied during the observed period. Figure 20 presents (in red) such interesting graph, with corresponding estimated error bars.

For the first days of observation – the lunar disc increasing its illuminated area as the phase was approaching full moon – the measured temperature was also increasing. However, the maximum temperature seems to be reached just past full moon (according to the plot, about 0.8 day after it [8]). The temperature curve also suggests a minimum about day 23.

Finally, Figure 21 represents published lunar temperature data obtained for similar frequencies (the wavelengths of 0.86, 1.25, and 3.15 cm respectively correspond to 35, 24, and 9.5 GHz) [23]. At least, the qualitative behaviour of the measured temperature coincides fairly well with such curves, as all of them show a phase lag. However, such real delay (about 3.5 days) is much larger than the found value (0.8 day).

[8] This quantitative value can be tricky, as (1) there are not enough values measured for that part of the curve, and (2) the red shown tendency line (4th order polynomial) is the one that better approximated among the few options that the used Microsoft Excel software allows. For instance, as there is also no sine curve alternative, the blue curve had to be represented by a 3rd order polynomial, which is clearly wrong after days 22-23 of Moon's cycle.

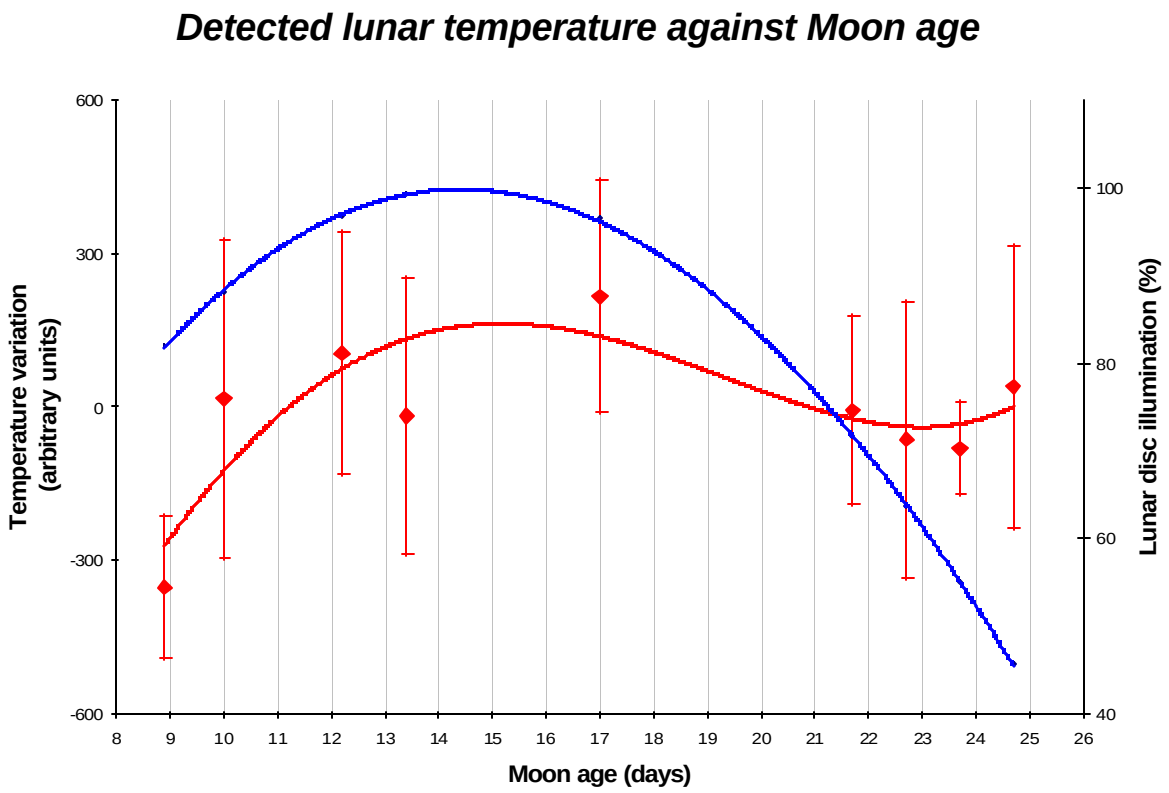

Figure 20
In red, the measured lunar temperature at 11.7 GHz, as a function of Moon age. In blue, the corresponding variation of the lunar disc illumination.

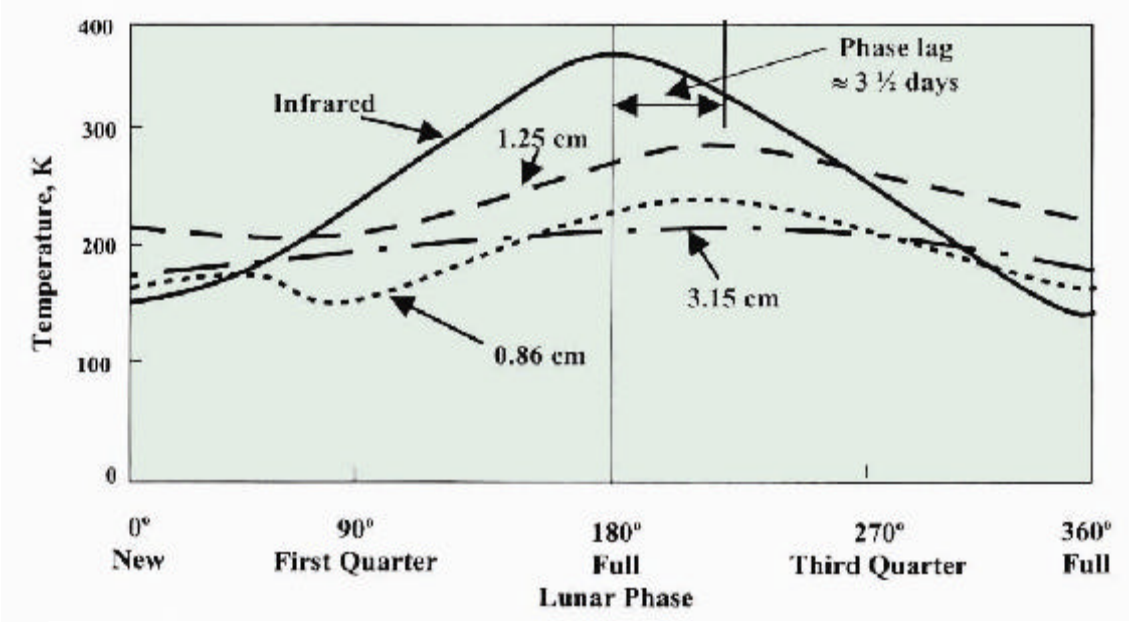

Figure 21
The real lunar temperature at different wavelengths, as a function of lunar phase.

Preliminary appraisal of built instruments

In order to properly assess the potential performance of the constructed instruments, it is firstly required to know as accurately as possible their basic parameters.

The 11.7 GHz radio telescope

1) Beamwidth

The first parameter to deal with, and also the easiest one, is the beamwidth (q). From the lunar plot of Figure 15, it was obtained a total lunar drift time of 683 seconds. Assuming that the Moon was moving at 14.4 degrees per hour[9], those 683 seconds mean 2.73 degrees.

From (1), $q = 1.019\frac{l}{D} = 1.019\ x\ \frac{0.0256}{0.95} = 0.0275$ rad = 1.57 degrees

Regarding that the diameter of the full covered area is actually twice the beamwidth, the total maximum expected drifting time becomes 3.14 degrees (which perfectly agrees with the measured value, considering that most likely the lunar disc has not exactly drifted by the centre of the beam dish). Thus, the acceptance covered by the 11.7 GHz dish is

$\Omega_{11.7\,GHz} = p\ q^2 = p\ x\ 0.0275^2 = 2.38\ x\ 10^{-3}$ sqr rad

2) Geometrical area of the dish

$A = p\ (D/2)^2 = p\ \ (0.95/2)^2 = 0.71\ m^2$

3) Solid angle subtended by the Moon

Considering that the average disc diameter of the Moon for the observing period was 32 arcmin, then

$\Omega_{moon} = p\ (32\ \text{arcmin}/2)^2 = p\ [(16/60)(p\ /180)]^2 = 6.81\ x\ 10^{-5}$ sqr rad

4) Ratio of lunar solid angular area to acceptance of the 11.7 GHz dish

$$R = \frac{\Omega_{moon}}{\Omega_{11.7GHz}} = \frac{6.81x10^{-5}}{2.38x10^{-3}} = 0.029$$

5) Flux density from the Moon at 11.7 GHz

From (7), and using an average T_{moon} = 213 K [23], then the flux density from the Moon becomes

[9] As it roughly takes about 25 hours for the Moon to pass at the same azimuthal direction.

$$F = \frac{2kT_{moon}\Omega_{moon}}{l^2} = \frac{2x1.38x10^{-23}x213x6.81x10^{-5}}{0.0256^2} = 6.11\ x\ 10^{-22}\ \text{W/Hz/m}^2$$

6) Antenna temperature of the Moon at the 11.7 GHz dish

From (4), it results

$$T_A = \frac{hAF}{2k} = \frac{0.5x0.71x6.11x10^{-22}}{2x1.38x10^{-23}} = 7.9\ \text{K}$$

7) System temperature for the Moon

The LNB alone has a noise figure of 0.7 dB, which is equal to a temperature noise of 50.7 K [24]. Estimating conservatory that losses in the feeder and line amplifier could add about 5 K, it becomes that $T_R \approx 56$ K. Then, for $T_{sky} \approx 3$ K, and $T_{ground} \approx 4$ K, from (8)

$$T_{sys(moon)} = T_A + T_R + T_{sky} + T_{gnd} \approx 7.9 + 56 + 3 + 4 = 71\ \text{K}$$

8) Gain

The total gain is from the LNB (65 dB), plus the line amplifier (20 dB) and the RF part of the modified satellite finder (17 dB), minus the losses of the coaxial cable (1.9 dB) and four F connectors (~ 1 dB each). This gives a total gain about 96 dB ($\approx 4x10^9$ times).

9) Voltage input before the diode detector due to the Moon

From (15), for $\Delta u = 500$ MHz, and for $R = 75$ ohm,

$$V_i = \sqrt{G.k.T_{sys}.\Delta u.R} = \sqrt{4x10^9\,x1.38x10^{-23}\,x71x5x10^8\,x75} = 0.38\ \text{V}$$

This result is an analytical verification of what was already known – that the lunar radio signal is strong enough for this radio telescope.

10) Measurement of the temperature system

The second parameter actually (although roughly) measured was the system temperature (T_{sys}). By pointing the dish at the ground, which acted as a noise source at ambient temperature (≈ 293 K), it was obtained a dc output of 10.32 V (measured with a digital tester). Then, by pointing the dish vertically at the sky (≈ 3 K) so that the spillover temperature were virtually zero, the corresponding measured value was 795 mV.

$$\frac{T_1 + T_{N1}}{T_2 + T_{N2}} = \frac{V_{O1}}{V_{O2}} \Rightarrow \frac{293 + T_{N1}}{3 + T_{N2}} = \frac{10.32}{0.795} = 12.98$$

Assuming $T_{N1} \approx T_{N2} = T_R$, then it results $T_R = 21$ K, which is about 40 % of the previously estimated value ($T_R \approx 56$ K). Anyway, this was a very crude measurement.

11) Minimum detectable temperature for the 11.7 GHz radio telescope

From (13), the resolution temperature becomes

$$\Delta T = \frac{T_N}{h\sqrt{t\Delta u}} = \frac{50.7+3}{0.5x\sqrt{0.1x5x10^8}} = 0.015 \text{ K}$$

12) Minimum detectable source flux density for the 11.7 GHz radio telescope

From (14),

$$S_{\min} = \frac{2k\Delta T}{A} = \frac{2x1.38x10^{-23}x0.015x10^{26}}{0.71} = 58 \text{ Jy}$$

The 1420 MHz eastern radio telescope

1) Beamwidth

For the 1420 MHz system, the correspondent l /D factor results 0.057, that is, 2.1 times greater than the l /D factor of the 11.7 GHz (0.027). Consequently, the beamwidth of the 1420 MHz radio telescope is about twice as large as of the 11.7 GHz (a predictable result after analyzing the graph of Figure 16).

2) Geometrical area of the dish

$A = p\ (D/2)^2 = p\ \ (3.7/2)^2 = 10.75 \text{ m}^2$

3) Antenna temperature of the Sun

From (4), and taking $F \approx 10^6$ Jy = 10^{-20} W/Hz/m^2 from Appendix V, it results

$$T_A = \frac{hAF}{2k} = \frac{0.5x10.75x10^{-20}}{2x1.38x10^{-23}} = 1947 \text{ K}$$

4) System temperature for the Sun

The LNA alone has a noise figure of 0.34 dB, which is equal to a temperature noise of 23.6 K [24]. Estimating conservatory that losses in the feeder and line amplifier could add about 5 K, it becomes that $T_R \approx 29$ K. Then, for $T_{sky} \approx 3$ K, and $T_{ground} \approx 4$ K, from (8)

$$T_{sys(moon)} = T_A + T_R + T_{sky} + T_{gnd} \approx 1947 + 29 + 3 + 4 = 1983 \text{ K}$$

5) Gain

The total gain is from the LNA (28 dB), plus the line amplifier (20 dB) and the RF part of the modified satellite finder (17 dB), minus the losses of the filter (3.8 dB), the coaxial cable (2.5 dB), four N and three F connectors (~ 1 dB each). This gives a total gain about 52 dB ($\approx 1.5x10^5$ times).

6) Voltage input before the diode detector due to the Sun

From (15), for Δu = 70 MHz, and R = 50 ohm,

$$V_i = \sqrt{G.k.T_{sys}.\Delta u.R} = \sqrt{1.5x10^5 x1.38x10^{-23} x1983x7x10^7 x50} = 0.0038 \text{ V}$$

This is exactly 100 times lesser than the same value for the Moon in the 11.7 GHz radio telescope, so that it now comes very clear why the 1420 MHz radio telescope is so noisy. Even for the Sun – the strongest radio source – the available signal before the detector diode is just too minute. It is required much more gain (at least, 40 dB more). That is the key that will definitively open the door towards the elusive fringes.

7) Minimum detectable temperature for the 1420 MHz radio telescope

The LNA has a noise figure of 0.34 dB ($\approx$23.6 K)

$$\Delta T = \frac{T_N}{h\sqrt{t\Delta u}} = \frac{23.6+3}{0.5x\sqrt{0.1x7x10^7}} = 0.020 \text{ K}$$

8) Minimum detectable source flux density for the 1420 MHz radio telescope

$$S_{\min} = \frac{2k\Delta T}{A} = \frac{2x1.38x10^{-23} x0.02x10^{26}}{10.75} = 5.1 \text{ Jy}$$

This is about one full order of magnitude lesser than for the 11.7 GHz system. In other words, the 1420 MHz radio telescope would have the potential of detecting radio signals about 10 times more feeble than its sibling instrument.

Discussion

Obtained results from the 11.7 GHz radio telescope were very stimulating, and far beyond expectations. The LNB has proved to be a truly low noise element. A careful calibration is still to be done, which will permit accurate temperature measurements to be attempted.

The obtained partial plot of varying microwaves from the Moon at 11.7 GHz with the lunar cycle is very convincing. Such thermal radiation come not just from the surface but is an integral over the surface of the Moon down to a depth of several meters [25]. The variations in temperature of the lunar surface are naturally quite large from day to night, but several meters down the variation is much smaller. This fact has been properly observed.

Another clear outcome, also correct, is the detection that the maximum temperature does not correspond exactly with full moon, but after it. However, such maximum appears too close (almost one day after full moon) compared to published data (about 3.5 days). Collecting more data would have surely improved the accuracy of the measurement.

The strong signal level detected from the Moon – the real support for the quality of the lunar results obtained – means that other radio sources in the sky will also be observable with this simple radio telescope. Conversely to earlier assumptions, this instrument still has a great potential to be worthwhile investigated.

The short time available to complete this project (just three months) conspired to obtain more and better results. Regarding the 11.7 GHz radio telescope, it would have been very interesting to obtain lunar graphs for an entire Moon cycle. Regarding the 1420 MHz system, the technical difficulties which prevented full operation of the singles radio telescopes – let alone the phased array interferometer – have yet to be solved.

Two plans are already high on the agenda of this amateur observatory. First of all, to make the interferometer to properly operate, and secondly, to use the 4 GHz LNB that came with one 3.7 m dish to build another "simple" radio telescope. The Pandora's box of radio astronomy has been opened at this facility, and exactly like this it will remain.

Conclusions

Practical radio astronomy has to do with close examination of tiny elusive ripples riding above an entire sea of noise. It is not an easy and straightforward activity to embark on – like amateur optical astronomy certainly is. Clearly, the author was excessively optimistic at the time of commitment to this project, basically due to his ignorance about the subject.

Just a little more than three months ago, practical radio astronomy was a totally unknown field for the author. Now, at least the fundamentals for designing and using single dish radio telescopes have become well understood. Considering that that was precisely the main objective for undertaking this project, the endeavour has been highly rewarding.

Certainly, amateur radio astronomy can be promissory attempted from backyards. As demonstrated, stimulating results can be readily obtained with off-the-shelf components. Excitement is guaranteed. It just requires a serious, strong-willed approach.

Acknowledgement

The author wishes to particularly express his thankfulness for the good practical advices and permanent support received alongside this project from Prof. Trevor Hill, from England. Having noticed that Prof. Hill is a well known expert in the field of design, construction, and use of small radio telescopes, the author had emailed him just to ask for some advices, and ended up with an invaluable and uninterested close collaboration, materialized in literally several dozens of exchanged emails.

References

[1] Trevor Hill, private communication (email of August 12, 2007)
[2] Kristen Rohlfs: *"Tools of Radio Astronomy"*. Springer-Verlag, 1986, page 76
[3] *"Understanding SRT Sensitivity"* at
http://www.haystack.mit.edu/edu/undergrad/srt/SRT%20Projects/ActivitySRTsensitiv
[4] John D. Kraus: *"Radio Astronomy"*, 2nd ed. Cygnus-Quasar Books, 1986, chapters 3, 6 & 7
[5] Jason Edwin Koglin: "Blackbody Temperature of the Sun at 4 GHz", at
http://www.astro.columbia.edu/~koglin/papers/solar.htm
[6] C R Kitchin: *"Astrophysical Techniques"*, 3rd ed. IoP Publishing Ltd, 2002, page 93
[7] Juan Aparici: *"A Wide Dynamic Range Square-Law Diode Detector"*. IEEE Transactions on Instrumentation and Measurements, Vol 37, No. 3, September 1988
[8] "Observations at 12 GHz" at http://perso.orange.fr/rulivas/shf.htm
[9] Trevor Hill, private communications (emails of September 9, 10, & 13, 2007)
[10] Ravinder S. Bhatia, Javier Marti-Canales, Clovis de Matos, Berndt Fritzsche, Frank Haiduk, and Uwe Knoechel: *"A Simple Radio Telescope Operating at Ku Band for Educational Purposes"*. IEEE Antennas and Propagation Magazine, Vol 48, No. 5, October 2006
[11] William Lonc: *"Radio Astronomy Projects"*, 3rd ed. Radio-Sky Publishing, 2006, pages 134-138
[12] *75 ohm coaxial cables* at: http://www.accesscomms.com.au/Specs/y8040spec.pdf
[13] Trevor Hill, private communications (emails of August 7, 9, 12, 12, & 14, 2007)
[14] *"Troubleshooting Your MAX186 ADC"* at
http://www.radiosky.com/skupipehelp/troubleshooting_max186_adc.html
[15] "The SkyPipe User Data Source (UDS) Model" at
http://radiosky.com/skypipehelp/UDS_model.html
[16] Ashley K. Wheeler: *"REU Summer 2006: KSU SRT (Small Radio Telescope) Project"* at
www.phys.ksu.edu/personal/leyjfk6/New%20Page%202_files/REU%20Paper.doc
[17] Trevor Hill: *"Radio Interferometry"*. Physics Education, Vol 28, Issue 4, July 1993, p243-247
[18] Danielle M. Lucero: *"N^2I^2: The New Mexico Tech and NRAO Instructional Interferometer"* at
http://www.nrao.edu/epo/amateur/N2I2.pdf
[19] *50 ohm coaxial cables* at http://home.alphalink.com.au/~gfs/products/dfb.htm
[20] Trevor Hill, private communication (email of October 3, 2007)
[21] John D. Kraus: *"Radio Astronomy"*, 2nd ed. Cygnus-Quasar Books, 1986, page 6-60
[22] Trevor Hill, private communication (email of October 23, 2007)
[23] John D. Kraus: *"Radio Astronomy"*, 2nd ed. Cygnus-Quasar Books, 1986, page 8-55
[24] John Fielding: *"Amateur Radio Astronomy"*. Radio Society of Great Britain, 2006, page 282
[25] Christian Monstein: *"The Moon's Temperature at l = 2.77 cm"*. Radio Astronomy and Plasma Physics Group, ETH Zurich, ORION 4/2001, August 2001, ISSN 0030-557X

All photos, plots, and diagrams were done by the author.

Appendix I

The modified satellite finder

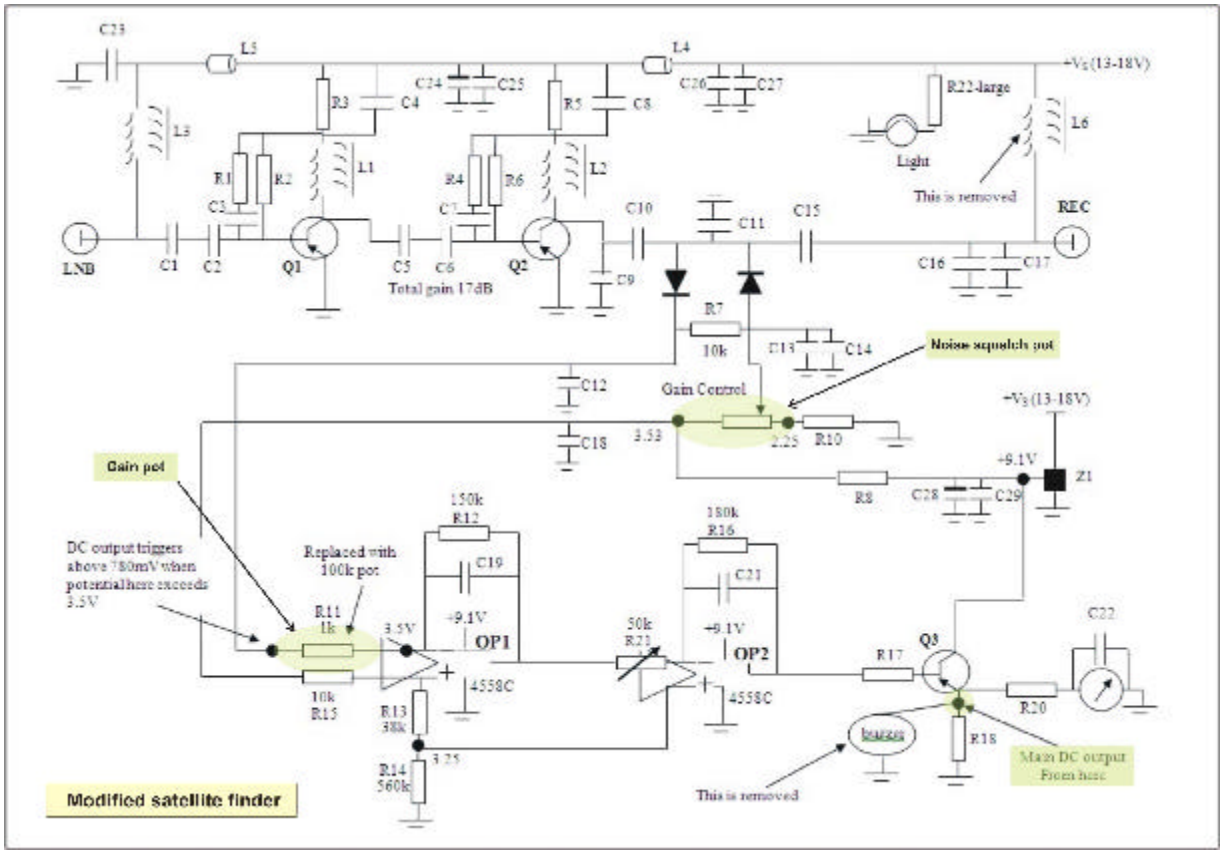

Several modifications were performed on the original circuit of the satellite finder device. The main ones are the addition of a new potentiometer (the "gain pot", at bottom left) that allows obtaining a fine variable dc output and, of course, the access to the dc output itself.

This simple but efficient circuit includes a system noise elimination facility (or squelch control) in the detector stage. This eliminates the bulk of the dc signal due to the noise generated primarily in the previous amplifiers, especially at the LNB. However, it does not eliminate the fluctuations in this noise signal caused by small random temperature changes of the electrons in the previous amplifier components. This latter variation causes the well known hiss in out-of-tune radio receivers, referred to as *white noise*.

Appendix II

The constructed 1420 MHz half wave dipole

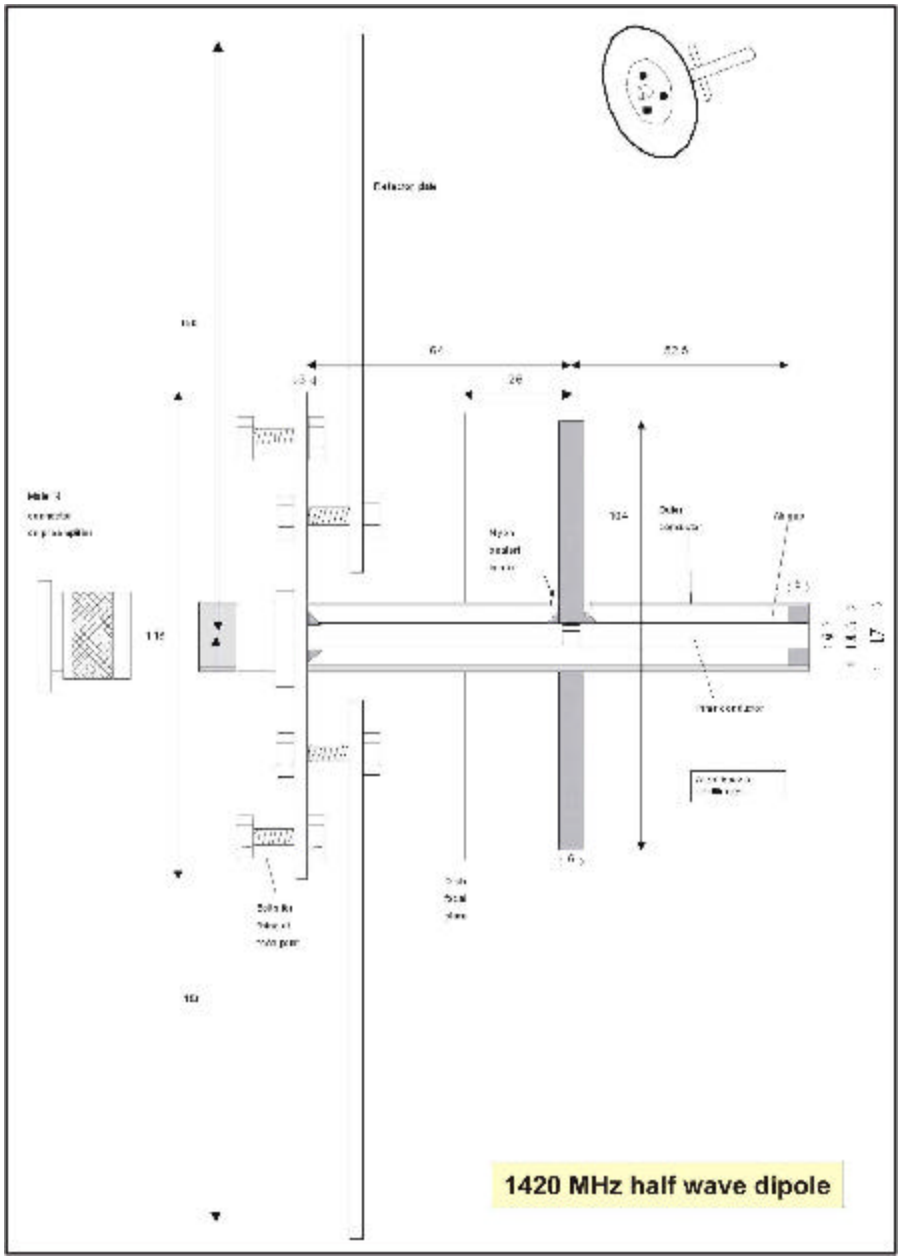

The resonant length of a half wave dipole is always slightly less than exactly half a wavelength, normally about 98 % of the actual length. The resonant frequency is 1420.4MHz (21.1 cm), so that 98% of the half wave is about 10.4 cm. This is the reason explaining the total length of the dipole, and the distances from the dipole to the backing plate and to end of the supporting bar (the crucial dimensions).

Appendix III

The constructed 1420 MHz resonant mechanical filter

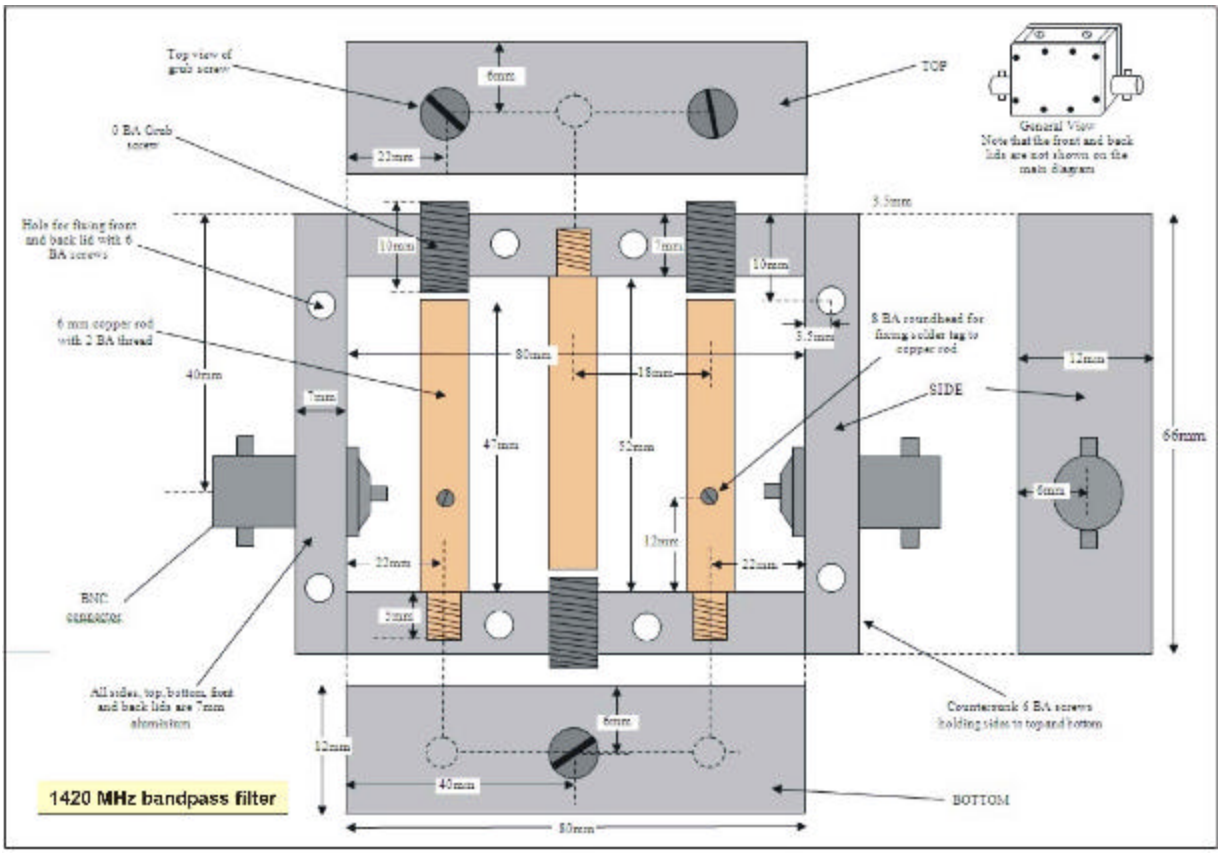

In pink, the copper rods. All the remaining pieces are aluminium. After the proper tuning at 1420 MHz, the air gap between the fixed rods and the screwed rods resulted about 0.2 mm.

Appendix IV

The strongest astronomical radio sources

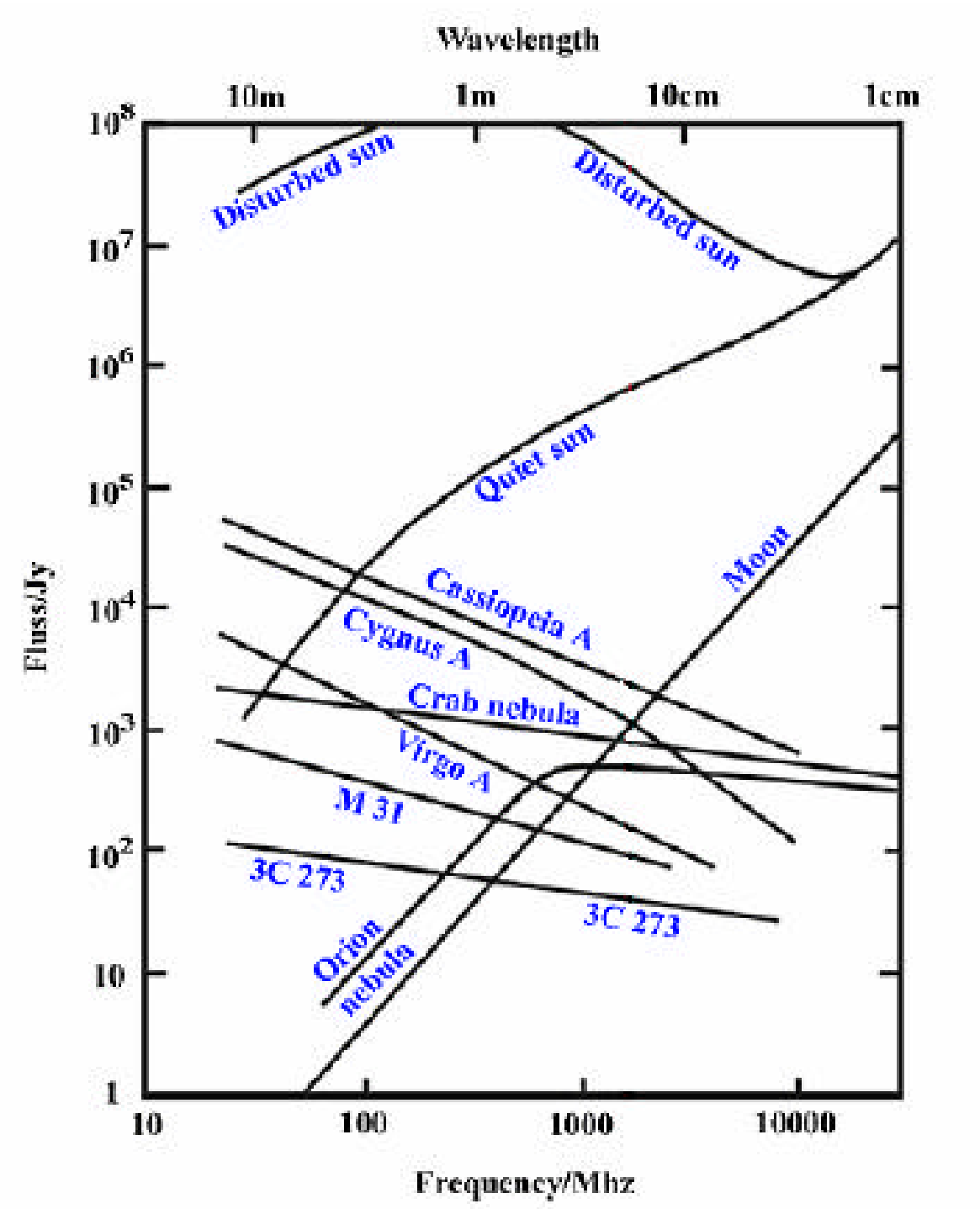

Appendix V

Total valid obtained data from lunar graphs

Date	UT Time of the maximum	Moon coordinates Azimuth	Moon coordinates Altitude	Disc illum. (%)	Angular size (arcmin)	Moon age (days)	Total time (sec)	Base (mV)	Maximum voltage (mV)	Half Max voltage (mV)	FWHM (sec)
2007-10-20	21:17:59	68° 35,344'	60° 50,876'	66,23	32	8,9	702	782	2603	1693	371
2007-10-20	21:44:40	60° 13,355'	65° 50,284'	66,35	32	8,9	680	790	2630	1710	399
2007-10-21	22:43:47	46° 35,341'	63° 22,359'	76,62	32	10,0	867	783	2860	1822	401
2007-10-21	23:06:54	35° 42,523'	66° 29,312'	76,71	32	10,0	1024	780	3779	2280	464
2007-10-23	23:13:54	52° 37,692	42° 20,350'	92,94	33	12,2	496	776	2312	1544	280
2007-10-23	23:47:42	43° 27,128'	47° 27,969'	93,04	33	12,2	564	777	2551	1664	312
2007-10-24	00:03:37	38° 30,460'	49° 35,118'	93,08	33	12,2	577	775	2454	1615	313
2007-10-24	00:21:34	32° 24,981'	51° 41,265'	93,13	33	12,2	1076	777	3065	1921	362
2007-10-24	23:54:37	48° 52,138'	35° 16,039'	97,88	34	13,4	811	772	2586	1679	387
2007-10-25	00:13:46	44° 18,565'	38° 05,517'	97,91	34	13,4	807	776	3667	2222	445
2007-10-25	00:31:44	39° 40,398'	40° 31,446'	97,94	34	13,4	804	776	3353	2065	428
2007-10-25	00:52:11	33° 56,283'	42° 59,744'	97,97	34	13,4	1307	790	3609	2200	480
2007-10-28	03:11:16	32° 36,559'	24° 09,794'	93,87	34	17,0	662	778	2641	1710	361
2007-10-28	04:05:46	20° 31,707'	29° 05,381'	93,71	34	17,0	721	779	3401	2090	381
2007-10-28	04:24:06	16° 07,795'	30° 14,419'	93,66	34	17,0	983	788	3597	2193	424
2007-11-01	09:45:03	356° 39,397'	35° 35,186'	55,40	32	21,7	831	766	3155	1961	389
2007-11-01	10:17:07	347° 51,370'	34° 46,641'	55,26	32	21,7	788	783	2729	1756	410
2007-11-01	10:35:02	343° 04,656'	33° 53,535'	55,18	32	21,7	707	789	3020	1905	358
2007-11-02	11:04:12	347° 28,790'	39° 31,894'	44,48	31	22,7	853	781	3539	2160	446
2007-11-02	11:39:37	337° 16,250'	37° 24,384'	44,33	31	22,7	611	782	3095	1939	449
2007-11-02	11:58:40	332° 07,294'	35° 46,052'	44,24	31	22,7	1188	787	4029	2408	508
2007-11-02	12:56:38	318° 12,730'	29° 00,885'	43,96	31	22,8	872	784	2922	1853	416
2007-11-03	10:43:02	08° 39,875'	45° 14,004'	34,53	31	23,7	799	783	3436	2110	402
2007-11-03	11:10:36	359° 15,298'	45° 44,269'	34,42	31	23,7	853	774	2710	1742	384
2007-11-03	11:34:06	351° 12,367'	45° 25,018'	34,33	31	23,7	777	770	2802	1786	409
2007-11-04	11:02:06	18° 32,338	49° 39,952'	25,28	30	24,6	742	778	3335	2057	382
2007-11-04	12:25:34	346° 25,761'	50° 47,140'	24,99	30	24,6	652	779	2893	1836	355
2007-11-04	12:44:04	339° 32,768'	49° 43,101'	24,92	30	24,7	856	783	2986	1885	417
2007-11-04	13:08:25	331° 03,991'	47° 40,137'	24,83	30	24,7	835	776	3516	2146	460
2007-11-04	13:29:24	324° 22,879'	45° 23,327'	24,75	30	24,7	686	777	2909	1843	395